

# Noise and conversion performance of a high- $T_c$ superconducting Josephson junction mixer at 0.6 THz

Xiang Gao,<sup>1,a)</sup> Jia Du,<sup>1</sup> Ting Zhang,<sup>2</sup> and Yingjie Jay Guo,<sup>2</sup>

<sup>1</sup>Commonwealth Scientific and Industrial Research Organization (CSIRO) Manufacturing, Lindfield, New South Wales, 2070, Australia

<sup>2</sup>Global Big Data Technologies Centre, University of Technology Sydney, Ultimo, New South Wales, 2007, Australia

This letter presents both theoretical and experimental investigations on the noise and conversion performance of a high- $T_c$  superconducting (HTS) step-edge Josephson-junction mixer at the frequency of 0.6 THz and operating temperatures of 20 to 40 K. Based on the Y-factor and U-factor methods, a double-sideband noise temperature of around 1000 K and a conversion gain of -3.5 dB were experimentally obtained at 20 K. At the temperature of 40 K, the measured mixer noise and conversion efficiency are around 2100 K and -10 dB, respectively. The experimental data are in good agreement with the numerical analysis results using the three-port model. A detailed performance comparison with other reported HTS terahertz mixers has confirmed the superior performance of our presented mixer device.

The non-linear property of Josephson junctions has been utilized for implementing various active devices (e.g. detectors, mixers) at the frequencies from microwave to terahertz (THz) band. For sub-millimeter and THz wave applications, due to the limited transmitting power and severe atmospheric absorption attenuation,<sup>1</sup> the system receivers are required to be extremely sensitive and thus capable of detecting the weak arriving signals. High- $T_c$  superconducting (HTS) Josephson-junction mixers<sup>2-7</sup> have been shown to be promising candidates for THz receiver frontends considering their high sensitivity, low noise, low local oscillator (LO) power requirement, and relatively cheaper cryogenic costs compared to that for cooling low- $T_c$  superconducting (LTS) devices.

So far, there has been very limited progress in experimental demonstrations of high performance HTS THz mixers due to the difficulty in fabricating reliable and reproducible HTS Josephson junctions. In addition, it is difficult to experimentally characterize the noise performance of the mixers at THz bands. A double-sideband (DSB) noise temperature of 1200 K was reported at operating temperature of 4.2 K for a thin-film antenna-coupled  $\text{YBa}_2\text{Cu}_3\text{O}_{7-\delta}$  (YBCO) step-edge Josephson junction mixer in the 0.3-THz band.<sup>2</sup> A 115-GHz waveguide mixer based on a single-grain-boundary bicrystal junction was measured to have a noise temperature of 1090 K at 10 K.<sup>3</sup> Scherbel *et al.*<sup>4</sup> reported a 345-GHz HTS Josephson mixer operating at 20 K with the noise temperature and conversion efficiency of 1003 K and -1.2 dB respectively. The above results, however, were achieved in a very low temperature range ( $T \leq 20$  K) where either liquid helium or very expensive bulky cryogenic instruments are required to cool the devices. The noise characterizations for HTS mixers at higher temperatures were reported at millimeter-wave band.<sup>8</sup> Theoretical methods have been developed for analyzing the noise and conversion performance of the LTS Josephson-junction mixers.

Amongst the methods, the three-port model developed by Taur<sup>9</sup> has been widely used for predicting low- $T_c$  Josephson mixer performance. Recently, Malnou *et al.* have applied this model to predict the conversion efficiency of their HTS THz mixer.<sup>5</sup>

In this Letter, we present the theoretical and experimental characterizations of a broadband antenna-coupled HTS Josephson-junction mixer, recently developed at our laboratory,<sup>7</sup> operating at the 0.6-THz band. The theoretical analysis is based on the three-port model approach, while the experimental measurement utilizes the Y-factor and U-factor methods. We shall show that very good agreement has been achieved between the simulated and measured results, including the DC current-voltage characteristics (IVCs), mixer noise temperature, and frequency down-conversion gain. Finally, a detailed performance comparison of our presented device with other reported HTS THz mixers is provided, which confirms that the superior mixer performance has been achieved at comparable frequencies and operating temperatures in this work.

Figure 1 illustrates the equivalent circuit for our HTS Josephson-junction THz mixer. It consists of a current bias and LO pumping circuits, a three-port model including the signal, image (non-negligible parasitic oscillation) and intermediate-frequency (IF) networks, as well as a resistively shunted junction (RSJ) model with a noise source<sup>9</sup>. Considering our presented device is a DSB THz mixer, the source impedances for the signal, image and LO are considered the same and equal to the input impedance  $Z_A$  of the thin-film antenna integrated with the Josephson junction. The radiation performance of the antenna had been optimized using the software Computer Simulation Technology (CST) Microwave Studio.<sup>7</sup> By taking advantage of the log-periodic impedance fluctuation characteristics, the  $Z_A$  was tuned as small as  $(40.6 + 2.2j) \Omega$  at the operating frequency of 0.6 THz

<sup>a)</sup> Electronic mail: Xiang.Gao@csiro.au

for reducing the antenna-junction mismatch. In addition, the IF microwave readout network had been designed for matching to  $50 \Omega$ . The details of the electromagnetic design for our presented mixer were previously reported.<sup>7</sup> The noise calculation and measurement described in this letter is at the fundamental mixing mode. First, the three-port model method<sup>9</sup> was employed to solve a noise-driven nonlinear pump equation in the time domain for obtaining the frequency-conversion and noise-correlation matrices. The second step was to solve a set of linear circuit equations formed by the matrices in the frequency domain to obtain the mixer noise and conversion gain. The numerical simulations were carried out by using the MATLAB software.

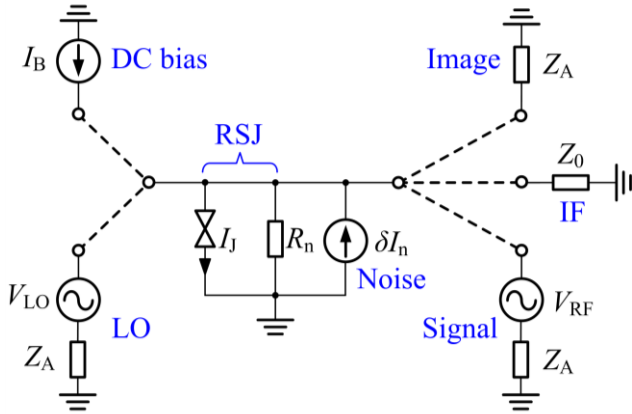


FIG. 1. Equivalent circuit of a HTS Josephson-junction THz mixer. Left: DC bias and LO pumping circuits; right: a three-port model including the signal, image and IF networks; middle: a HTS RSJ model with a noise source. Dashed lines were used to indicate the external circuits are connected to the junction terminals with good port isolations between each other. Partial simulation parameters:  $R_n = 4.4 \Omega$ ,  $Z_A = (40.6 + 2.2j) \Omega$ , and  $Z_0 = 50 \Omega$ .

The HTS THz mixer chip was implemented using the CSIRO established step-edge YBCO junction technology<sup>10</sup> and more details of device fabrication and module packaging can be found in Ref. [7]. Figure 2 illustrates the experimental set-up for mixer noise and conversion gain characterizations. The inset is a micrograph of the fabricated mixer device, showing the microwave matching circuit and the thin-film log-periodic antenna integrated with a  $2\text{-}\mu\text{m}$  wide YBCO step-edge Josephson junction at its geometrical center. A  $0.6\text{-THz}$  LO pumping signal, generated from a Virginia Diodes Inc. (VDI) solid-state source and guided by a pair of off-axis parabolic mirrors, is combined via a beam splitter with the THz noise signal radiated by a hot ( $295\text{ K}$ ) or cold ( $77\text{ K}$ ) blackbody, and coupled into the mixer module mounted in a cryocooler. Here, the hot blackbody was implemented by placing a piece of THz absorber in a container at room temperature ( $295\text{ K}$ ), while the cold load was realized by pouring liquid nitrogen into the container until the absorber was immersed. The combined two THz signals (LO and noise) were coupled onto the Si lens attached on the back of the mixer chip through the cryocooler window. A quasi-optical filter and an infrared (IF) film were placed in front of the cryocooler window for external interference rejection. A

fundamental heterodyne mixing occurs at appropriate biasing, provided by a battery-operated current source. The down-converted IF signal was amplified by a cryogenic low noise amplifier (LNA) followed by a room-temperature (RT) LNA. An IF filter with the central frequency of  $2.365\text{ GHz}$  and bandwidth of  $390\text{ MHz}$  was used after the RT amplifier. An HP 438A power meter, with input overload protection, was used for recording the IF signal. The total gain and input noise for the whole IF link was calibrated to be approximately  $50\text{ dB}$  and  $14\text{ K}$ , respectively.

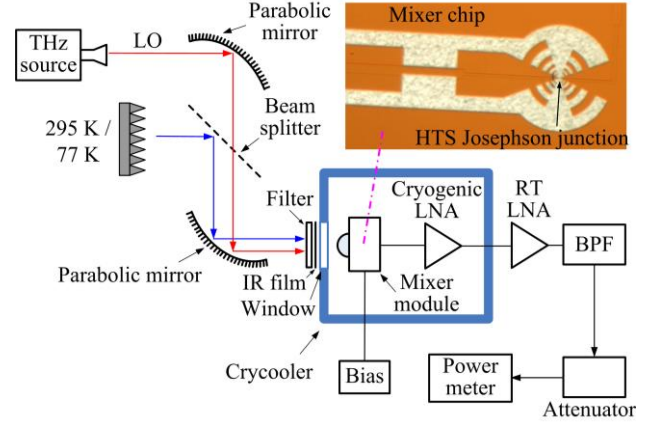


FIG. 2. Schematic showing an experimental set-up for the noise temperature and conversion gain characterizations. Inset is a micrograph of the fabricated mixer chip showing the thin-film antenna, matching circuit and HTS Josephson junction.

The DSB noise temperature  $T_{\text{mix}}$  and conversion gain  $G_{\text{mix}}$  of the HTS THz mixer can be obtained from the measured IF output power by using the so-called Y-factor and U-factor methods.<sup>11-12</sup> Specifically, the formula of  $T_{\text{mix}}$  can be derived from Eqs. (4) and (5) in Ref. [11], while the  $G_{\text{mix}}$  is determined by referring to Eq. (1) in Ref. [12] but with a minor modification here. The isolator termination introduced thermal noise was removed as there was no isolator used between the mixer module and cryogenic amplifier in our set-up (see Fig. 2). The formulas are summarized as follows:

$$T_{\text{mix}} = \frac{T_{\text{hot}} - Y_1 T_{\text{cold}}}{L_{\text{opt}} (Y_1 - 1)} - \frac{T_{\text{hot}} (L_{\text{opt}} - 1)}{L_{\text{opt}}} \quad (1)$$

$$G_{\text{mix}} = \frac{L_{\text{opt}} T_{\text{IF}} U (Y_2 - 1)}{2 Y_2 (T_{\text{hot}} - T_{\text{cold}})} \quad (2)$$

where  $L_{\text{opt}}$  is the quasi-optical loss,  $T_{\text{IF}}$  is the input noise of the IF link,  $T_{\text{hot}}$  and  $T_{\text{cold}}$  are the equivalent temperatures of a blackbody according to the Callen-Welton definition<sup>13</sup> at  $295\text{ K}$  and  $77\text{ K}$ , respectively. In addition, the factors  $Y_1$ ,  $Y_2$  and  $U$  are defined as

$$Y_1 = (P_{\text{IF, hot}} - P_{\text{IF, sc}}) / (P_{\text{IF, cold}} - P_{\text{IF, sc}}) \quad (3)$$

$$Y_2 = P_{\text{IF, hot}} / P_{\text{IF, cold}} \quad (4)$$

$$U = P_{\text{IF, hot}} / P_{\text{IF, sc}} \quad (5)$$

where  $P_{\text{IF, hot}}$  and  $P_{\text{IF, cold}}$  are the measured IF output power for the mixer coupling blackbody radiations at 295 K and 77 K, respectively, and  $P_{\text{IF, sc}}$  is the IF output noise floor when the mixer operates in the superconducting state (neither DC bias nor LO pumping is applied).

Figure 3 shows the simulated and measured DC current-voltage characteristics (IVCs) of the presented HTS mixer at the operating temperatures of 20 K and 40 K. The Josephson junction displays an obvious RSJ behavior with a normal resistance  $R_n$  of 4.4  $\Omega$ . The junction critical current  $I_c$  is 520  $\mu\text{A}$  at 20 K and 370  $\mu\text{A}$  at 40 K. When the HTS mixer is illuminated by a 0.6-THz LO signal, the  $I_c$  is partly suppressed and a series of Shapiro steps appear on the IVCs. Those induced steps are resulted from the resonance effect between the external THz pumping and internal Josephson oscillation. As clearly shown in Fig. 3, the voltage at the first Shapiro step  $V_1$  and the LO signal frequency  $f_{\text{LO}}$  comply well with the theoretical relationship<sup>14</sup>  $V_1 = \Phi_0 f_{\text{LO}}$  (where  $\Phi_0$  is the magnetic flux quantum). The LO pumping power  $P_{\text{LO}}$  was estimated to be  $\sim -35$  dBm, which was obtained from measuring the THz LO signal induced  $I_c$  suppression and Shapiro current step-height plus deducting the junction-antenna impedance mismatch loss. From Fig. 3, the measured IVCs are in good agreement with that of the numerical simulation.

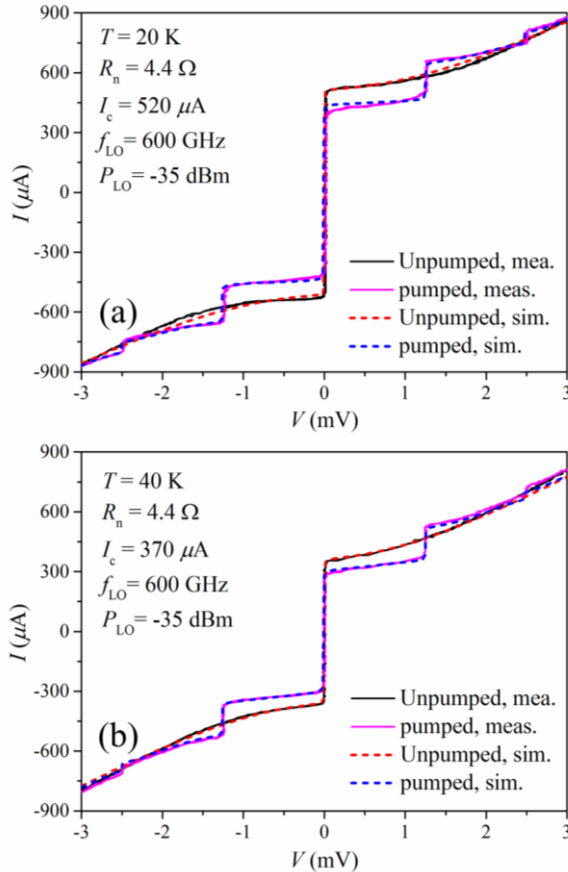


FIG. 3. Simulated and measured DC IVCs at the temperatures of (a) 20 K and (b) 40

K.

By using the experimental set-up shown in Fig. 2, we have characterized the noise temperature and conversion gain of our HTS mixer at the temperatures of 20 and 40 K. As shown in Fig. 4(a), the measured IF power  $P_{\text{IF}}$  versus bias  $I_B$  traces for the hot and cold blackbody conditions (in red and blue respectively) at  $T = 20$  K show obvious output peaks at around 450  $\mu\text{A}$ , an optimal bias current (locating about halfway between the zeroth and first Shapiro step of the pumped IVC shown in Fig. 3 (a)). Using the measured  $P_{\text{IF, hot}}$ ,  $P_{\text{IF, cold}}$  and  $P_{\text{IF, sc}}$  (about 5.5 nW for a bath temperature of 20 K), the DSB noise temperature  $T_{\text{mix}}$  and mixer conversion gain  $G_{\text{mix}}$  were obtained using Eqs. (1) - (5), and the results are shown in Figs. 4(a) and 4(b). A best  $T_{\text{mix}}$  of  $1000 \pm 60$  K and  $G_{\text{mix}}$  of  $-3.5 \pm 0.2$  dB were achieved. The experimental results agree well with the calculated ones (the dashed lines). Some minor discrepancies are expected due to the measurement errors and slight variation of quasi-optical calibration. On the whole, the theoretical and measured results (Fig. (4)) showed very good consistency, indicating the good performance of our presented HTS THz mixer.

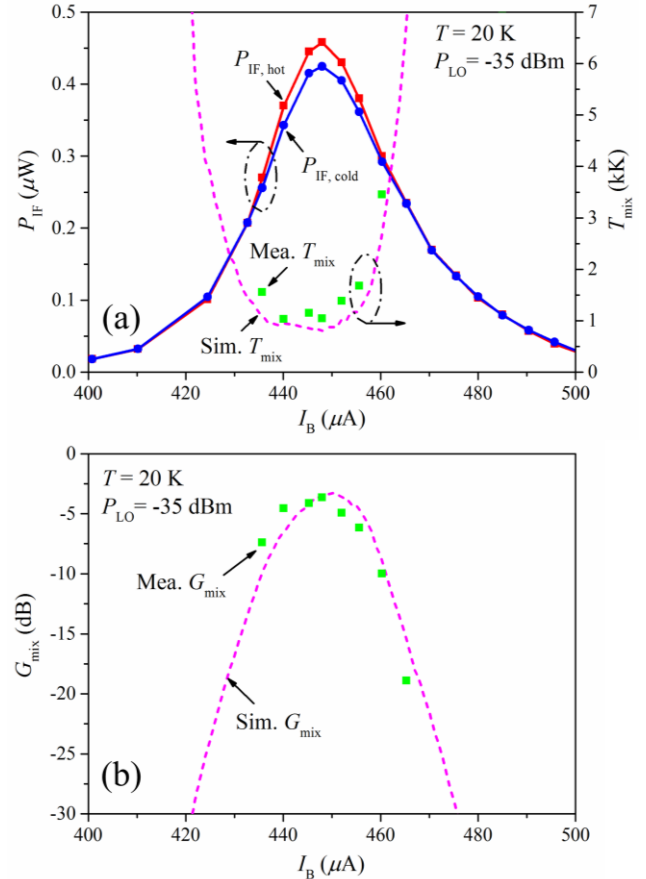


FIG. 4. (a) Measured  $P_{\text{IF}}$  versus  $I_B$  for the hot and cold blackbody conditions and the obtained DSB noise temperature, compared to the simulated result (dashed line); (b) measured mixer conversion gain compared to the simulated result (dashed line).

Figure 5 shows the simulated and measured  $T_{\text{mix}}$  and  $G_{\text{mix}}$  values as the function of LO pumping power,  $P_{\text{LO}}$ , at 20

K and 40 K. For each value of  $P_{LO}$ , a corresponding optimal bias current has been applied to the mixer. The experimentally obtained noise temperature  $T_{mix}$  and conversion gain  $G_{mix}$  are  $2100 \pm 200$  K and  $-10 \pm 0.4$  dB at  $T = 40$  K. These values are close to that predicted by the simulated results. The simulation showed that the device performance is influenced by the LO power although the change is not as sharp as that of the bias ( $I_B$ ) dependence. In this experiment, the  $P_{LO}$  was fixed at  $-35$  dBm, which was a bit lower than the optimal LO pumping power shown in Fig. 5. A better mixer performance, i.e. lower  $T_{mix}$  and higher  $G_{mix}$ , could be achieved if the LO (THz) power could be increased somewhat by improving our current quasi-optical set-up. Obviously, the mixer performance also improves with lowering the bath temperatures. Seen from Fig. 5, the optimal LO pumping occurs at  $P_{LO} \approx -30$  dBm or  $1 \mu\text{W}$ , which is much lower than that required for Schottky diode mixers.<sup>15</sup> This is one of the advantages of the Josephson-junction mixer.

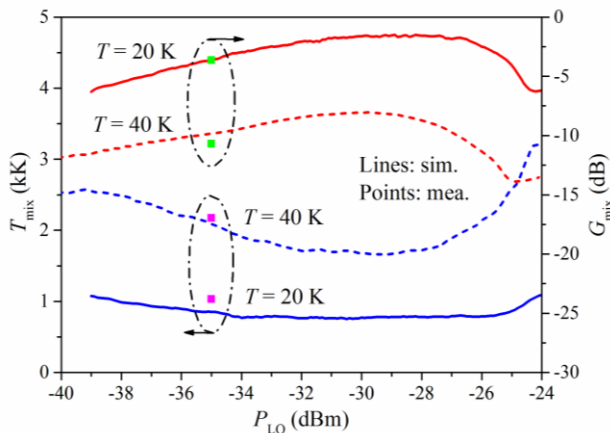


FIG. 5. Simulated and measured  $T_{mix}$  &  $G_{mix}$  versus  $P_{LO}$  for 20 K and 40 K operating temperatures.

TABLE I. Performance comparison for typical HTS THz mixers

References	Operating frequency	Operating temperature	Conversion gain	Noise temperature
[2]	300 GHz	4.2 K	---	1200 K
[3]	115 GHz	10 K	-10.1 dB	1090 K
[4]	345 GHz	20 K	-1.2 dB	1003 K
[5]	140 GHz	58 K	-40 dB	---
This work	600 GHz	20 K	-3.5 dB $\pm 0.2$ dB	1000 K $\pm 60$ K
		40 K	-10 dB $\pm 0.4$ dB	2100 K $\pm 200$ K

The experimental results can be reliably reproduced with minimum variations (within reasonable measurement errors). We did, however, find out that it is very important to keep the environmental influences to the minimum during the experiment. As shown in Fig. 2, we applied an IR film and

THz filter in front of the mixer/cryocooler window to eliminate the unwanted thermal noise, infrared and other interferences from the environment. Moreover, we placed the absorber inside a well-defined metal container to minimize the environment caused uncertainty and kept the blackbody entirely stationary during the experiment while changing the hot- and cold-load.

A detailed performance comparison between the presented device and other reported HTS THz mixers is given in Table I. It can be observed that our mixer shows a superior performance at the comparable frequencies and operating temperatures. The mixer in Ref. [4] has a slightly higher conversion gain at 20 K, but its operating frequency is much lower than that of our device. Generally, the performance of an HTS mixer deteriorates as the operating frequency or temperature rises. We have not seen any reports of the noise and conversion gain characterizations of HTS mixers at the 600 GHz frequency band. The superior performance of our presented HTS THz mixer is attributed to the excellent characteristics of our step-edge Josephson junction and careful electromagnetic simulation designs. Finally, it should be mentioned that the device performance could be further improved if applying a little more LO power (as indicated by Fig. 5).

In conclusion, we have presented theoretical and experimental investigations for the noise and conversion performance of our antenna-coupled step-edge HTS Josephson-junction mixer at 0.6 THz. The measured results agree well with that obtained by numerical simulation. Operating in a fundamental mixing mode, the presented mixer device demonstrated a DSB noise temperature of around 1000 K at  $T = 20$  K and 2100 K at  $T = 40$  K, and a corresponding conversion gain of  $-3.5$  dB and  $-10$  dB, respectively. The numerical calculation has predicted that further improvement in performance is possible if the mixer is pumped by a higher power LO signal. The presented HTS THz heterodyne mixer can be potentially applied in THz wireless communication or sensing front-end systems.

<sup>1</sup>G. Ducournau, P. Szeftgiser, F. Pavanello, E. Peytavit, M. Zaknounge, D. Bacquet, A. Beck, T. Akalin, and J.-F. Lampin, *J. Infrared Millimeter THz Waves* **36**, 198 (2015).

<sup>2</sup>H. Shimakage, Y. Uzawa, M. Tonouchi, and Z. Wang, *IEEE Trans. Appl. Supercond.* **7**, 2595 (1997).

<sup>3</sup>O. Harnack, M. Darula, J. Scherbel, J.-K. Heinsohn, M. Siegel, D. Diehl, and P. Zimmermann, *Supercond. Sci. Technol.* **12**, 847 (1999).

<sup>4</sup>J. Scherbel, M. Darula, O. Harnack, and M. Siegel, *IEEE Trans. Appl. Supercond.* **12**, 1828 (2002).

<sup>5</sup>M. Malnou, C. Feuillet-Palma, C. Ulysse, G. Faini, P. Febvre, M. Sirena, L. Olanier, J. Lesueur, and N. Bergeal, *J. Appl. Phys.* **116**, 074505 (2014).

<sup>6</sup>J. Du, A. R. Weily, X. Gao, T. Zhang, C. P. Foley, and Y. J. Guo, *Supercond. Sci. Technol.* **30**, 024002 (2017).

<sup>7</sup>X. Gao, T. Zhang, J. Du, A. R. Weily, Y. J. Guo, and C. P. Foley, *Supercond. Sci. Technol.* **30**, 095011 (2017).

<sup>8</sup>O. Harnack, M. Darula, S. Beuven, and H. Kohlstedt, *Appl. Phys. Lett.* **76**, 1764 (2000).

- <sup>9</sup>Y. Taur, IEEE Trans. Electron Devices **ED-27**, 1921 (1980).
- <sup>10</sup>C. P. Foley, E. E. Mitchell, S. K. H. Lam, B. Sankrithyan, Y. M. Wilson, D. L. Tilbrook, and S. J. Morris, IEEE Trans. Appl. Supercond. **9**, 4281 (1999).
- <sup>11</sup>D. Liu, J. Li, Z. Wang, M. Yao, J. Hu, and S. C. Shi, IEEE Trans. Appl. Supercond. **23**, 1400504 (2013).
- <sup>12</sup>S. Cherednichenko, M. Kroug, H. Merkel, P. Khosropanah, A. Adam, E. Kollberg, D. Loudkov, G. Gol'tsman, B. Voronov, H. Richter, and H.-W. Huebers, Physica C **372-376**, 427 (2002).
- <sup>13</sup>A. R. Kerr, IEEE Trans. Microw. Theory Tech. **47**, 325 (1999).
- <sup>14</sup>T. V. Duzer and C. W. Turner, *Principles of Superconductive Devices and Circuits* (Prentice-Hall, Upper Saddle River, NJ, USA, 1999).
- <sup>15</sup>[Http://www.vadiodes.com](http://www.vadiodes.com).